Penerbit Akademia Baru

Journal of Advanced Research in Fluid Mechanics and Thermal Sciences

Journal homepage: www.akademiabaru.com/arfmts.html
ISSN: 2289-7879

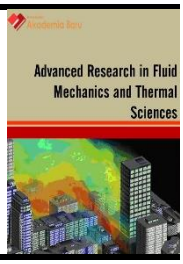

Unsteady MHD Boundary Layer Flow and Heat Transfer of Ferrofluids Over A Horizontal Flat Plate with Leading Edge Accretion

Open Access

Sayyid Zainal Abidin Syed Ahmad[1,2], Wan Azmi Wan Hamzah[2,3,*], Mohd Rijal Ilias[1], Sharidan Shafie[1], Gholamhassan Najafi[4]

[1] Department of Mathematical Sciences, Faculty of Science, Universiti Teknologi Malaysia, 81310 Johor Bahru, Malaysia
[2] Faculty of Mechanical Engineering, Universiti Malaysia Pahang, 26600 Pekan, Pahang, Malaysia
[3] Automotive Engineering Centre, Universiti Malaysia Pahang, 26600 Pekan, Pahang, Malaysia
[4] Tarbiat Modares University, Tehran, Iran

ARTICLE INFO

Article history:
Received 12 September 2018
Received in revised form 12 May 2019
Accepted 20 May 2019
Available online 18 July 2019

ABSTRACT

The unsteady forced convection boundary layer flow of ferrofluids past a semi-infinite flat plate is theoretically investigated. The governing equations are transformed into uncoupled ordinary differential equations using similarity transformation. Similarity equations were solved numerically by employing the Fourth-Fifth Order Runge-Kutta Felhberg method with shooting technique. MAPLE software was used in order to obtain graphical results. This study investigates the behavior of water and kerosene suspension which contains nanoparticles of magnetite (Fe_3O_4) together with heat transfer analysis due to boundary layer flow. In this problem, a comparison between two different base fluids mixed magnetic particle; Fe_3O_4-water and Fe_3O_4-kerosene has been conducted. The impact of different types of volume fraction on heat transfer enhancement and fluid flow characteristics together with the effect of several leading edge and magnetic field parameters has been studied. The effects of various physical parameters on the velocity profiles, temperature profiles, skin friction and Nusselt number were investigated numerically. The obtained results of this paper are compared to regular fluid without magnetic effect and the comparison shows good agreement with the published results. It is found that, the ferrofluids velocity, temperature and heat transfer rate increases with an increase magnetic field and nanoparticles volume fraction.

Keywords:
Ferrofluid; Boundary layer flow; Heat transfer; MHD; Runge-Kutta Felhberg method

Copyright © 2019 PENERBIT AKADEMIA BARU - All rights reserved

1. Introduction

Heat transfer plays an important role for a real life application as where technological advances development. The determination of the rates of such energy transfers is called heat transfer which is form of energy which passes from a body at higher temperature to a body at a lower temperature.

* *Corresponding author.*
E-mail address: wanazmi2010@gmail.com (Wan Azmi Wan Hamzah)

There are present in the thermal equipment used in many engineering applications and produced by all the major industrial sectors. At the moment, heat transfer enhancement is a major concern especially in the field of thermal engineering. Thus, efforts need to be put to improve the heat transfer performance of thermal devices used. Heat transfer improvement can be made by increasing (i) heat transfer area, (ii) temperature, and (iii) heat transfer coefficient [1]. However, technologies have already reached their limit for the cases (i) and (ii). There are three fundamental modes of heat transfer; conduction, convection and radiation. In this work, convection was selected as type of heat transfer. Heat transfer which can travel through a medium and also through vacuum between solid or moving fluid is called convection. Heat transfer due to convection involves the energy exchange between a surface and an adjacent fluid.

Almost a century ago, boundary layer plays a significant role in determining accurately the flow of certain fluids. Boundary layer concept has developed in 1904 by Ludwig Prandtl. The theory concept was based on observations in wind tunnel experiments. According to Prandtl's hypothesis, the effects of fluid friction at high Reynolds number are limited to a thin layer near the boundary body known as boundary layer term. The significance of Prandtl theory lies in the simplification that it allows in the analytical treatment of viscous flow theory. The solution to boundary layer flows is obtained from the reduced "Navier Stokes" equations for which boundary layer assumptions and approximations have been applied. The solution to these equations was obtained in 1908 by Blasius, a student of Prandtl's. He has begun with the exact solution method by performed a transformation technique to change the set of two coupled partial differential equations into a single ordinary differential equation. He solved the boundary layer over a flat plate in external flows. Callegari and Friedman [2] studied to develop an exact analytical solution to a basic problem of the boundary layer theory of viscous fluids. Specifically, a solution is presented for the classical problem which is incompressible flow of a uniform stream past a semi-infinite flat plate at zero incidences. Thus the only unknowns are the velocity components. Acrivos [3] studied the boundary layer flows for such fluids in 1960, since then a large number of related studies have been conducted because of their importance and presence of such fluids in chemicals, polymers, molten plastics, and others.

Recently many researchers found that dispersing nanosized particles into the liquids result in higher heat transfer coefficient of these newly developed fluids called nanofluids compared to the traditional liquids. Therefore, the term of nanofluids was introduced by Choi [4] who was working with the group at the Argonne National Laboratory (ANL), USA in 1995. The characteristic feature of nanofluids is thermal conductivity enhancement, a phenomenon observed by Masuda, Ebata and Teramae [5]. These fluids are engineered colloidal suspensions of nanoparticles in a base fluid. As a consequence, the nanofluids has reputed that it would be having a greater heat transfer rate compared with those common working base fluids such as water, ethylene glycol, kerosene and mineral oil. Nanofluids have become interesting for many researchers on the studied of applied nanofluids especially in the heat transfer equipment. Nanofluids are the new invented fluids that mixed of two substances; liquid and solid. The initial idea of the nanofluids is the improvement of the working fluids. Hence, the liquid substance of the nanofluids usually will be the common working fluids that widely used in the heat transfer industrial equipment such as aforementioned. The solid content in the nanofluids are called nanoparticles which has the size of range from 1 nm to 100 nm. Alam, Rahman and Sattar [6] investigated the similarity solutions for hydromagnetic free convective heat and mass transfer flow along a semi-infinite permeable inclined flat plate with heat generation and thermo-phoresis. Nanoparticles can be classified in metallic and non-metallic. The metallic types are divided into pure metal form and metal-oxide form. Magnetic of nanofluids become known as ferrofluids.

In recent years, ferrofluids has emerged as a new class of 'smart nanofluid', whose properties are controllable by an external magnetic field. It is well known for its unique property of having both liquid and magnetic properties. Ferrofluids is a magnetic colloidal suspension consisting of base liquid and magnetic nanoparticles with a size range of 5 to 15 nm in diameter coated with a surfactant layer. The most often used magnetic particle materials are magnetite, iron or cobalt; and the base liquids are water or kerosene. It can be controlled by both magnitude and direction of an external magnetic field and temperature [7]. Ferrofluids usually do not retain magnetization in the absence of an externally applied field [8]. One of the best types of magnetic material is ferromagnetic (Fe_3O_4) was selected in this study [9]. Ram and Kumar [10] noticed that temperature of the ferrofluids decreases with the increase of viscosity radiation parameter. It was found that temperature of the ferrofluids decrease with the increase of viscosity radiation parameter. Colla, Fedele, Scattolini and Bobbo [11] investigated water-based Fe_3O_4 nanofluid characterization of thermal conductivity, viscosity measurements and correlation. They have found the same results of viscosity variation with the temperature. Abareshi, Goharshadi, Zebarjad, Fadafan and Youssefi [12] have been studied fabrication, characterization and measurement of thermal conductivity of Fe_3O_4 nanofluids. Borglin, Moridis and Oldenburg [13] studied experimentally the flow of a ferrofluids in porous media. Therefore, the ferrofluids could be applied for various industrial fields especially enhancement and depression of the heat transfer such as electronic packing, mechanical engineering, smart fluids, thermal engineering, magnetic sealing, damping and bearing of machines, energy conversion system, aerospace, and bioengineering [14]. Other applications include magneto-optical wavelength filter, optical modulators, nonlinear optical materials, tunable optical fiber filter, optical grating, optical switches, drug targeting, drug delivery, MRI contrast, and hyperthermia.

Interestingly, so far no study has been reported in the literature to study the magnetohydrodynamics (MHD) for unsteady boundary layer flow and heat transfer of ferrofluids over flat plate with leading edge accretion. The study of MHD flow is the academic discipline concerned with the dynamics of electrically conducting fluids in a magnetic field. There has been a great interest in the study of MHD flow and heat transfer in any medium due to the effect of a magnetic field on the boundary-layer flow control and on the performance of many systems using electrically-conducting fluids. Based on the importance of ferromagnetic materials, Qasim, Khan, Khan and Ali Shah [15] examined MHD flow with slip condition in the presence of heat transfer in ferrofluid over a stretched cylinder with given heat flux. They used water as conventional base fluid and added magnetite (Fe_3O_4) nanoparticles. Khan, Khan, Qasim and Shah [16] tackled a stagnation point problem of ferrofluids along a stretching sheet with viscous dissipation and heat transfer. Malvandi, Kaffash and Ganji [17] investigated the theoretical study on effects of nanoparticles migration on magnetohydrodynamic mixed convective heat transfer of alumina/water nanofluid inside a vertical microchannel. They insist by applying a magnetic field leads to 42% and 30% increase in the values of heat transfer rate for small and large nanoparticles respectively. Besides that, Sheremet, Pop and Roşca [18] have discussed numerically about magnetic field effect on the unsteady natural convection in a wavy-walled cavity filled with a nanofluid. That stated increase in the magnetic parameter number leads to an attenuation of convective flow and heat transfer and then produce a formation of a double-core convective cell. Pourmehran, Rahimi-Gorji and Ganji [19] reported that heat transfer and flow analysis of nanofluid flow induced by a stretching sheet in the presence of an external magnetic field.

This type of flow has attracted the interest of many researchers due to its application in many engineering problems such as MHD generators, plasma studies, nuclear reactors, crystal growth, and geothermal energy extractions [20]. Therefore, it is of great interest to study the effects of magnetic

field and other participating parameters on the temperature distribution and heat transfer when the fluid is not only an electrically conducted.

2. Methodology

2.1 Mathematical Formulation

The problem considered is an unsteady laminar two-dimensional convection flow of ferrofluids past a static horizontal flat plate with leading edge accretion. This study also assumed incompressible and the viscous dissipation and radiation effects are neglected. The fluids are water and kerosene based ferrofluid containing magnetite (Fe_3O_4) as a ferroparticle. The base fluid (water and kerosene) and the ferroparticle are in thermal equilibrium and no slip occurs between them. Assume the distance from the origin is defined as $B(x) = B_0 / \sqrt{((\cos\alpha)\tau + \sin\alpha)}$ with $B_0 \neq 0$ where $((\cos\alpha)\tau + \sin\alpha)$ is the coordinate along the plate and B0 is the magnetic field strength. The y-axis runs along the free stream direction and the x-axis is perpendicular to it. A transverse magnetic field of strength B0 is applied in x-direction normal to the plate with the assumption that the magnetic Reynolds number is small, so that the induced magnetic field can be neglected as compared to the applied magnetic field. Hence, the applied magnetic field contributes only to the Lorentz force which acts in the x-direction. Plate was taken along the x-axis and y-axis was taken as normal to the flow direction as shown in Figure 1.

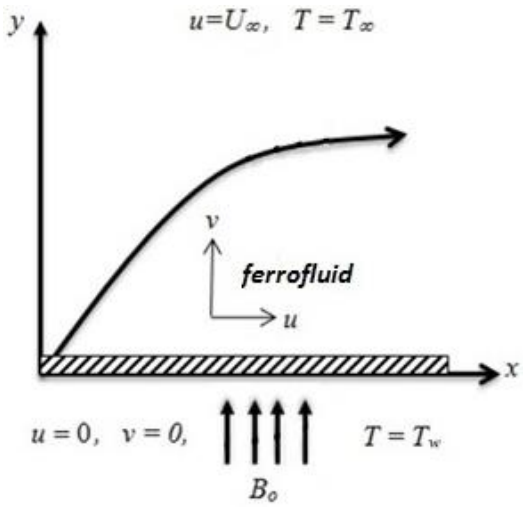

Fig. 1. Physical model and coordinates system

Under above assumptions along with the assumptions of the Boussinesq and boundary layer approximations, the basic continuity, momentum and thermal energy governing equation of ferrofluid in the presence of magnetic field over a horizontal flat plate are given by others [21-24] and stated in Eq. (1) to (3).

$$\frac{\partial u}{\partial x} + \frac{\partial v}{\partial y} = 0 \tag{1}$$

$$\frac{\partial u}{\partial t} + u\frac{\partial u}{\partial x} + v\frac{\partial u}{\partial y} = \nu_{nf}\frac{\partial^2 u}{\partial y^2} - \frac{\sigma B^2(x)(u - U_\infty)}{\rho_{nf}} \tag{2}$$

$$\frac{\partial T}{\partial t}+u\frac{\partial T}{\partial x}+v\frac{\partial T}{\partial y}=\alpha_{nf}\frac{\partial^2 T}{\partial y^2}. \tag{3}$$

Subject to the boundary conditions for the static plate case.

$$\begin{aligned} &u(x,0)=0,\ v(x,0)=0,\ T(x,0)=T_w,\\ &u(x,\infty)=U_\infty \text{ and } T(x,\infty)=T_\infty. \end{aligned} \tag{4}$$

where u is the fluid velocity in x-direction, v is the fluid velocity in y-direction, ν_{nf} is the effective kinematic viscosity of the ferrofluid, σ is the electrical conductivity, U∞ is the free stream velocity, ρ_{nf} is the effective density of the ferrofluid, T is the temperature, T_w is the wall temperature, T∞ is the free stream temperature and α_{nf} is the thermal diffusivity of the ferrofluid which given as Eq. (5) [25, 26].

$$\begin{aligned} \mu_{nf}&=\frac{\mu_f}{(1-\phi)^{2.5}},\\ \rho_{nf}&=(1-\phi)\rho_f+\phi\rho_s,\\ \alpha_{nf}&=\frac{k_{nf}}{(\rho C_p)_{nf}},\\ (\rho C_p)_{nf}&=(1-\phi)(\rho C_p)_f+\phi(\rho C_p)_s. \end{aligned} \tag{5}$$

Here, ϕ is the solid volume fraction, μ_{nf} is the effective dynamic viscosity of the ferrofluid, μ_f is the dynamic viscosity of the base fluid, ρ_f and ρ_s are the densities of the base fluid and ferroparticle, $(\rho C_p)_{nf}$ is the effective heat capacity of the ferrofluid, $(\rho C_p)_f$ and $(\rho C_p)_s$ are the specific heat parameters of base fluid and ferroparticles, k_{nf} is the thermal conductivity of the ferrofluid, k_f and k_s is the thermal conductivities of the base fluid and ferroparticle. The effective thermal conductivity of the ferrofluid is approximated by Maxwell-Garnetts model in Eq. (6).

$$\frac{k_{nf}}{k_f}=\frac{(k_s+2k_f)-2\phi(k_f-k_s)}{(k_s+2k_f)+\phi(k_f-k_s)} \tag{6}$$

The stream function ψ(x,y) defined as

$$u=\frac{\partial\psi}{\partial y}\text{ and }v=-\frac{\partial\psi}{\partial x}, \tag{7}$$

that satisfies the continuity Eq. (1). Consider the stream function

$$\psi(x,y,t)=U_\infty\sqrt{(\cos\alpha)\nu_f t+(\sin\alpha)\left(\frac{\nu_f x}{U_\infty}\right)}\,f(\eta), \tag{8}$$

along the similarity variables

$$\eta=\frac{y}{\sqrt{(\cos\alpha)\nu_f t+(\sin\alpha)\left(\frac{\nu_f x}{U_\infty}\right)}}, \tag{9}$$

and dimensionless temperature

$$\theta(\eta)=\frac{(T-T_\infty)}{(T_w-T_\infty)}. \tag{10}$$

where α is the unsteady parameter of leading edge, ν_f is the kinematic viscosity of the base fluid, ψ is the stream function and $Re_x=\frac{U_\infty x}{\nu_f}$ is the Reynolds number.

Based on these definitions, the velocity can be written as Eq. (11).

$$u=U_\infty f'(\eta),$$
$$v=\frac{\left(\frac{\nu_f}{2}\right)(\eta f'-f)(\sin\alpha)}{\left((\cos\alpha)\nu_f t+(\sin\alpha)\left(\frac{\nu_f x}{U_\infty}\right)\right)^{\frac{1}{2}}}. \tag{11}$$

Using the variables in Eq. (8) to (11), the transformed Eq. (1) to (4) were reducing to the following nonlinear system of ordinary differential equations can be written as Eq. (12) and (13).

$$\frac{1}{(1-\phi)^{2.5}}\cdot\frac{1}{\left((1-\phi)+\phi\frac{\rho_s}{\rho_f}\right)}f'''+\frac{1}{2}(\cos\alpha)\eta f''+\frac{1}{2}(\sin\alpha)f''$$
$$-\frac{1}{\left((1-\phi)+\phi\frac{\rho_s}{\rho_f}\right)}M(f'-1)=0. \tag{12}$$

$$\frac{k_{nf}}{k_f}\theta''+\frac{\Pr}{2}\left((1-\phi)+\phi\frac{(\rho C_p)_s}{(\rho C_p)_f}\right)\left[(\cos\alpha)\eta+(\sin\alpha)f\right]\theta'=0. \tag{13}$$

The transformed boundary conditions (4) become

$$f(0)=0,\ f'(0)=0,\ \theta(0)=1,\ ,\\ f'(\infty)=1,\ \text{and}\ \theta(\infty)=0. \tag{14}$$

where primes denotes differentiation with respect to η, $\Pr=(\mu C_p)_f/k_f$ is the Prandtl number, $M=\sigma B_0^2/\rho U_\infty$ is the magnetic parameter.

Skin friction coefficient, C_f at the surface of the plate and local Nusselt number, Nux which are defined as Eq. (15).

$$C_f=\frac{\tau_w}{\rho_f U_\infty^2}, Nu_x=\frac{xq_w}{k_f(T_w-T_\infty)} \tag{15}$$

where τ_w is the skin friction or shear stress and q_w is the heat flux from the surface plate defined as Eq. (16).

$$\tau_w=u_{nf}\left(\frac{\partial u}{\partial y}\right)_{y=0}\ and\ q_w=-k_{nf}\left(\frac{\partial T}{\partial y}\right)_{y=0} \tag{16}$$

Substituting Eq. (8), (9), (10) and (11) into Eq. (15) and (16)

$$C_f(Re_x)^{\frac{1}{2}}=\frac{1}{(1-\phi)^{2.5}}\left(\frac{f''}{\sqrt{(cos\alpha)\tau+(sin\alpha)}}\right)and\\ Nu_x(Re_x)^{-\frac{1}{2}}=-\frac{k_{nf}}{k_f}\frac{\theta'(0)}{\sqrt{((cos\alpha)\tau+sin\alpha)}} \tag{17}$$

where $\tau=t\dfrac{U}{x}$ is the non-dimensional time variable introduced by Stewartson [27].

2.2 Solution of the Problem

The set of coupled higher order nonlinear differential Eq. (12) and (13) along with the boundary conditions of Eq. (14) which are formed a two point boundary value problem have been solved numerically by using the Fourth-Fifth Order Runge-Kutta-Fehlberg method by Aziz [28]. This method involves, transforming the equation into a set of initial value problems (IVP) which contain unknown initial values that need to be determined by guessing after which the fourth order Runga-Kutta Fehlberg iteration scheme is employed. Then, iteration scheme would be integrating the set of IVPs until the given boundary conditions are satisfied with established an adaptive numerical with shooting technique. Firstly, Eq. (12) and (13) subjects to the boundary conditions Eq. (14) are written in a system of first order system of equations. To fulfil this requirement, let's introduce new dependent variables are present as Eq. (18).

$$x_1=f, x_2=f', x_3=f'', x_4=\theta, x_5=\theta'. \tag{18}$$

By substituting Eq. (18) into Eq. (12) and (13) are then reduced to systems of first order differential equations are obtained;

$$x_3^{'} = -\frac{1}{2} x_3 (1-\phi)^{2.5} \left((1-\phi) + \phi \frac{\rho_s}{\rho_f} \right) \left[(\cos\alpha)\eta + (\sin\alpha) x_1 \right] + (1-\phi)^{2.5} M (x_1 - 1). \quad (19)$$

$$x_5^{'} = -x_5 \frac{k_f}{k_{nf}} \frac{\Pr}{2} \left((1-\phi) + \phi \frac{(\rho C_p)_s}{(\rho C_p)_f} \right) \left[(\cos\alpha)\eta + (\sin\alpha) x_1 \right]. \quad (20)$$

And initial conditions are transformed as follows

$$x_1(0) = 0, x_2(0) = 0, x_3(0) = s_1, x_4(0) = 1, x_5(0) = s_2 \quad (21)$$

In the shooting method, the unknown initial conditions s1 and s2 in Eq. (21) are assumed and first order Eq. (19) and (20) integrated numerically as an IVP to a given terminal point. The accuracy of the assumed missing initial conditions was checked by comparing the calculated value of the dependent variable at the terminal point with its given value. If differences exist, improved values of the missing initial conditions are obtained and the process repeated. An iteration method is then applied on the latter system to adjust the initial guess using the Newton method. The Newton approach is utilized to update the initial guesses until the asymptotic boundary conditions are reached. A step size of $\Delta\eta = 0.001$ was selected to be satisfactory for a convergence criterion of 10-7 in nearly all cases. The value of η∞ was found to each iteration loop by the assignment statement η∞ = η∞ + $\Delta\eta$. The maximum value of η∞ to each group of parameters with α, ϕ , M and Pr is determined when the values of unknown boundary conditions at η = 0 not change to successful loop with error less than 10-7. The computations were done by a program which uses a symbolic and computational computer language MAPLE by Heck [29]. Being a BVP, the equations are automatically solved by the "dsolve" command by applying the appropriate algorithm.

3. Results

For the analysis, the values of Prandtl number for the base fluids of water and kerosene are taken to be 6.2 and 21 respectively. The effect of the volume fraction of solid ferroparticle ϕ is studied in the range 0 ≤ ϕ ≤ 0.2, where ϕ = 0 represents the pure water or kerosene. The two types of base fluids containing ferroparticles of Fe_3O_4 are considered. The thermo-physical properties of water, kerosene and Fe_3O_4 are given in Table 1. Present results are compared with previous result for verification of accuracy based on the values of the rate heat transfer of skin friction C_f in the absence of a magnetic field (M = 0) and the leading edge parameter effects at α = 0° and 90°. The skin friction results of the present investigation were compared with previous authors such as Loganathan and Vimala [30], Blasius [31] and Cortell [32]; and found to be in good agreement as presented in Table 2 and Table 3. The comparison of the results with and without the MHD effect has shown in Table 4. From the table, magnetic field strength enhances the local skin friction for the model with MHD. Physically, this implies that the plate surface exerts a drag force on the fluid.

Table 1
Thermo-physical properties of base fluid and Ferro particles

Physical Properties	Water	Kerosene	Fe_3O_4
ϕ (kg/m³)	997.1	780	5200
Cp (J/kg.K)	4179	2090	670
k (W/m.K)	0.613	0.149	6

Table 2
Comparison of the skin friction coefficient C_f for different values of volume fraction of ferroparticles at (M=0) between two different using of base fluids

ϕ	Loganathan and Vimala [30] Cu-water (Pr=6.2)		Present Result Cu-water (Pr=6.2)		Present Result Fe_3O_4 - water (Pr=6.2)		Present Result Fe_3O_4 - kerosene (Pr=21)	
	α=0°	α=90°	α=0°	α=90°	α=0°	α=90°	α=0°	α=90°
0	0.5626	0.3321	0.5642	0.3319	0.5642	0.3319	0.5642	0.3319
0.05	-	-	0.7112	0.4184	0.6619	0.3894	0.6814	0.4009
0.1	0.8597	0.5075	0.8625	0.5075	0.7674	0.4515	0.8056	0.4739
0.15	-	-	1.0238	0.6024	0.8831	0.5196	0.9402	0.5532
0.2	1.1964	0.7066	1.2005	0.7063	1.0123	0.5956	1.0892	0.6408

Table 3
Comparison of the skin friction C_f for present result (water as base fluid) when fixed values of Pr=6.2, M=0, α=90° and ϕ=0

η	Present results	Blasius [31]	Cortell [32]
0.0	0.3319	0.3321	0.33206
1.0	0.3229	0.322	0.32301
2.0	0.2667	0.2668	0.26675
3.0	0.1614	0.1616	0.16136
4.0	0.0642	0.0642	0.06423
5.0	0.0159	0.0166	0.01591
6.0	0.0024	0.0024	0.00240
7.0	0.0002	0.000	0.00022

Table 4
Comparison of the skin friction coefficient C_f (without and with MHD) fordifference values of volume fraction of ferroparticles between two different base fluids

α=90°	Volume fraction	(M=0)	(M=1)
Fe_3O_4-water (Pr=6.2)	0.01	0.3432	1.05912
	0.1	0.4515	1.21298
	0.2	0.5956	1.43109
Fe_3O_4-kerosene (Pr=21)	0.01	0.3456	1.05979
	0.1	0.4739	1.22061
	0.2	0.6408	1.44882

In order to bring out the important features of the flow and the heat transfer characteristics, the numerical results are presented in Figure 2 to 9. A detailed discussion on the effects of the governing parameters, namely prandtl number Pr, magnetic field M, volume fraction ϕ and leading edge α as

prescribed parameters. The velocity, temperature, skin friction coefficient and local Nusselt number are carried out in this section.

3.1 Velocity Profiles

Figure 2 has shown the effect of magnetic field with overall of leading edge on the velocity $f'(\eta)$ in the case of Pr = 6.2 (Fe_3O_4 - water) and Pr = 21 (Fe_3O_4 - kerosene) when M = 1. It can be seen that the velocity profiles have the same result as above but the difference is leading edge. When the magnetic parameter increases from 1 to 3, leading edge at 0° have influence the velocity at the highest value but decrease in momentum boundary layer thickness becomes mostly a thin layer. In contact with leading edge situation, it reveals the normal aligned (at α = 0°) is the better way where the streamlines are moving.

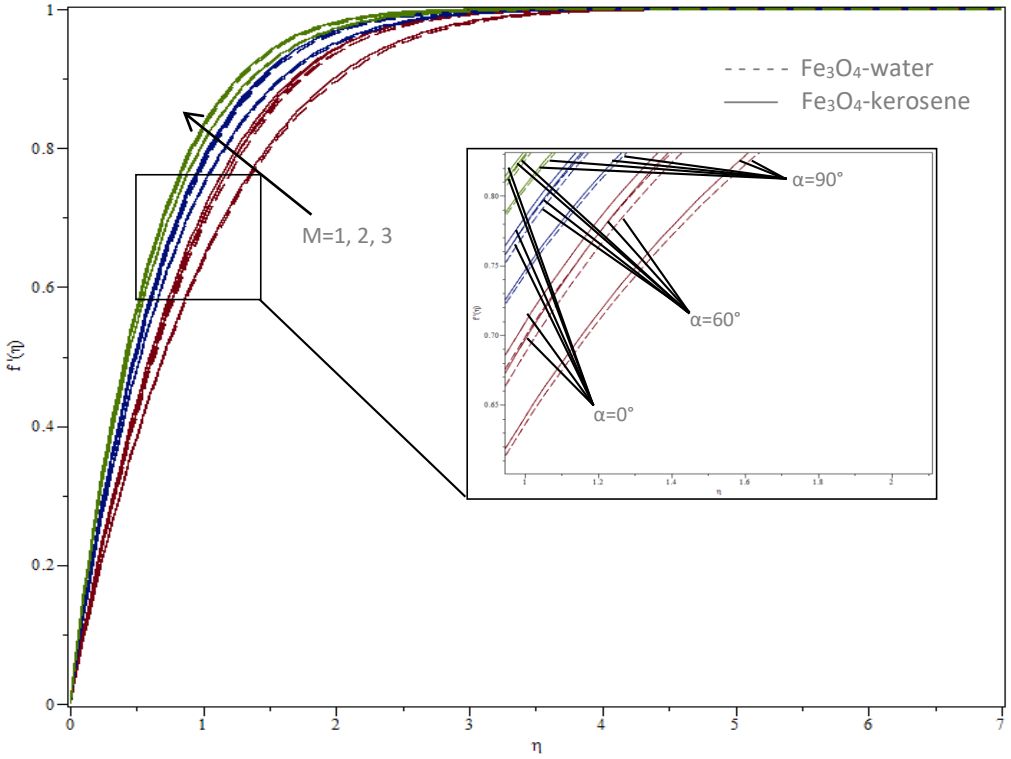

Fig. 2. Velocity profile f' (η) along η for various values of magnetic field, M at Pr=6.2 and 21, α=0°, 60° and 90°, ϕ =0.1

Figure 3 has shown the effect of volume fraction with overall of leading edge on the velocity $f'(\eta)$ in the case of Pr = 6.2 (Fe_3O_4 - water) and Pr = 21 (Fe_3O_4 - kerosene) when M = 1. It can be seen that the velocity profiles have the same result as above but the difference is leading edge. When the volume fraction increases from 0 to 0.2, leading edge at 0° have influence the momentum boundary layer thickness to become highest value. In contact with leading edge situation, it reveals the normal aligned (at α = 0°) is the better way where the streamlines are moving.

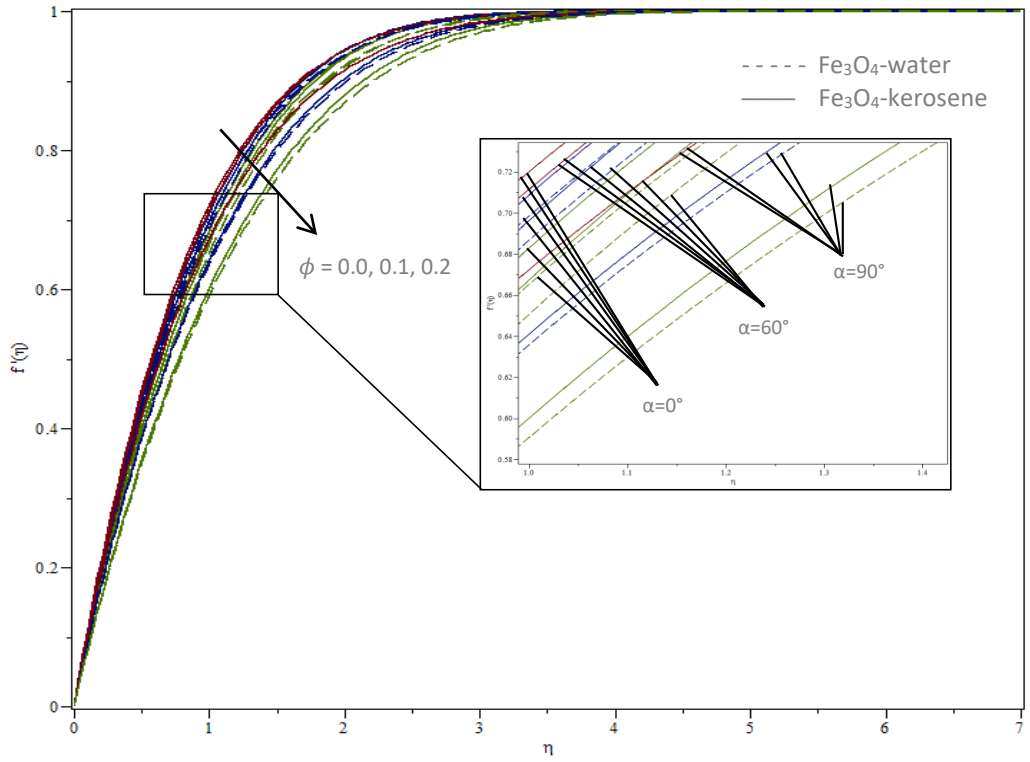

Fig. 3. Velocity profile f' (η) along η for various values of volume fraction, ϕ at Pr=6.2 and 21, α=0°, 60° and 90°, M=1

Figure 4 has shown the effect of the leading edge on the velocity profiles f' (η) in the case of Pr = 6.2 (Fe_3O_4 - water) and Pr = 21 (Fe_3O_4- kerosene) when M=1, ϕ =0.1. It can be seen that the rate of flow velocity is considerably decrease with the increase of leading edge, α. That means the velocity of Fe_3O_4 - kerosene always become higher than Fe_3O_4 - water for each leading edge and velocity at α=0° of Fe_3O_4 - kerosene has become the highest value compare two others at α=60° and α=90°. By the increase of leading edge, it has increased the momentum boundary layer thickness.

3.2 Temperature Profiles

Figure 5 shown the effect of magnetic field with overall of leading edge on the temperature profiles $\theta(\eta)$ in the case of Pr = 6.2 (Fe_3O_4 - water) and Pr = 21 (Fe_3O_4 - kerosene) when M = 1. It can be seen that the temperature profiles have the same result as above but the difference is leading edge. When the magnetic parameter increases from 1 to 3, at α = 90° is the highest value that increase more in thermal boundary layer thickness. In contact with leading edge situation, it reveals the normal aligned (at α = 90°) is the better way where the streamlines are moving.

Figure 6 has shown the effect of volume fraction with overall of leading edge on the temperature profiles in the case of Pr = 6.2 (Fe_3O_4 - water) and Pr = 21 (Fe_3O_4 - kerosene) when M = 1. It can be seen that the temperature profiles have the same result as above but the difference is leading edge. When the volume fraction increases from 0 to 0.2, at α = 90° is the highest value that increases thermal boundary layer thickness. In contact with leading edge situation, it reveals the normal aligned (at α = 90°) is the better way where the streamlines are moving.

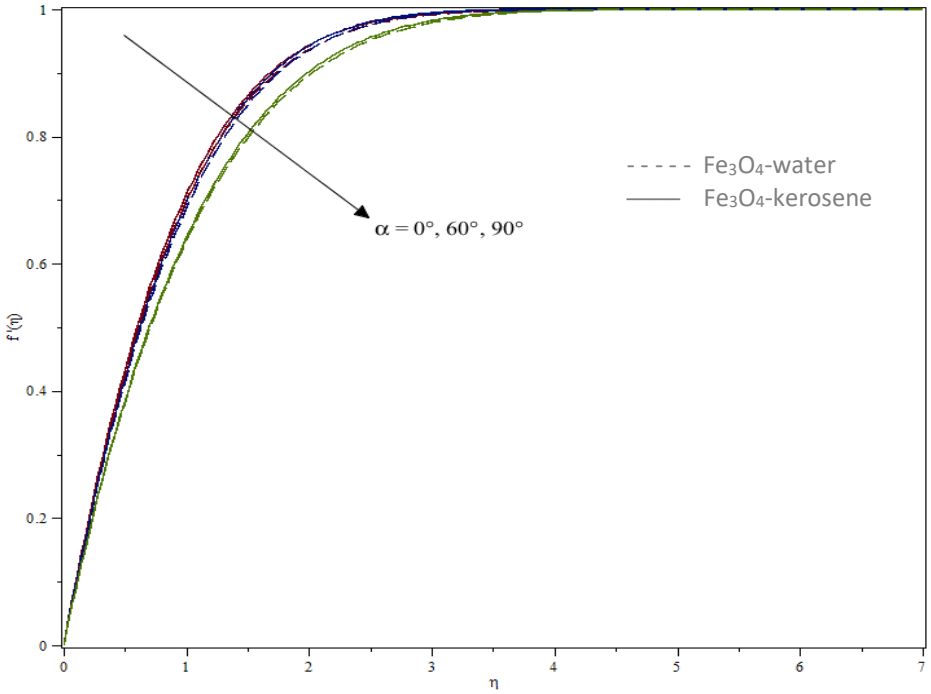

Fig. 4. Velocity profile f' (η) along η for various values of leading edge, α at Pr=6.2 and 21, M=1, ϕ =0.1

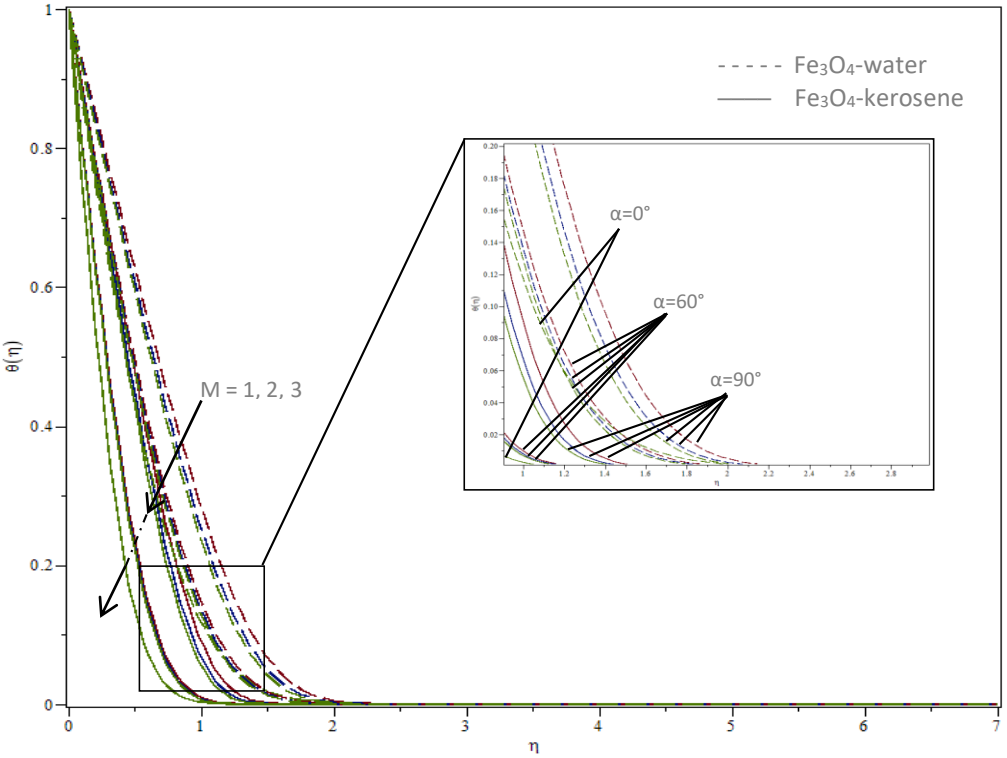

Fig. 5. Temperature profile θ (η) along η for various values of magnetic field, M at Pr=6.2 and 21, α=0°, 60° and 90°, ϕ =0.1

Figure 7 has shown the effect of the leading edge on the temperature profiles θ (η) in the case of Pr = 6.2 (Fe_3O_4 - water) and Pr = 21 (Fe_3O_4 - kerosene) when M=1, ϕ =0.1. It can be seen that the rate of flow temperature is considerably increase with the increase of leading edge, α. In other hand, the temperature of Fe_3O_4 - water always become higher than Fe_3O_4 - kerosene for each leading edge and

temperature at α=90° of Fe_3O_4 - water has become the highest value compare two others at α=0° and α=60°. By increase of leading edge, it has increased the thermal boundary layer thickness.

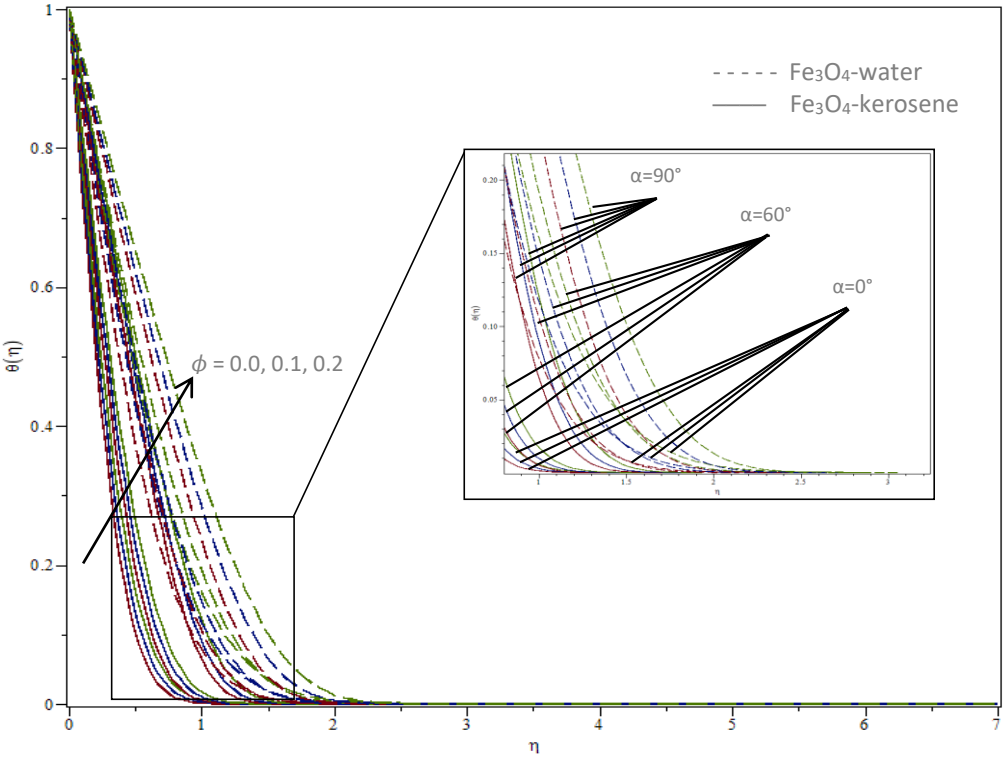

Fig. 6. Temperature profile θ (η) along η for various values of volume fraction, ϕ at Pr=6.2 and 21, α=0°, 60° and 90°, M=1

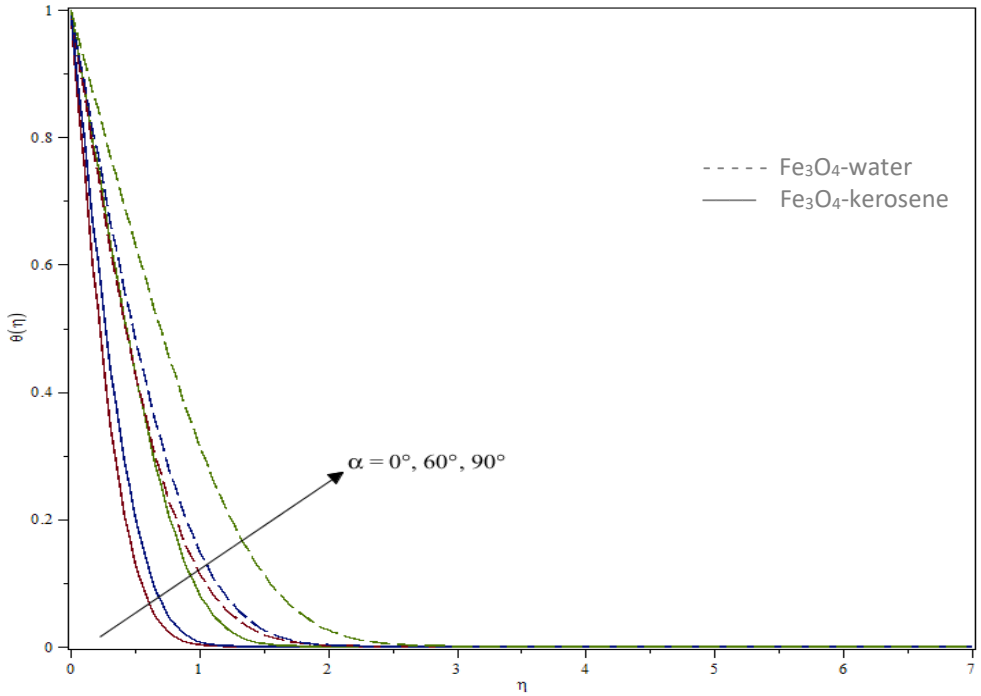

Fig. 7. Temperature profile θ (η) along η for various values of leading edge, α at Pr=6.2 and 21, M=1, ϕ =0.1

Physically, it is noted in those figures as a conjunction Fe_3O_4 – kerosene has been recorded gain the best result in velocity profile compared to Fe_3O_4– water. Based on results, kerosene provides a larger Prandtl number that would affect to velocity and temperature behaviour. When Prandtl number is large, decrement of temperature of Fe_3O_4 – kerosene transferred slowly due to increment isothermal lines. However, for small Prandtl number, heat is transferred slower. Meanwhile, magnetite particle gives a reason that, it can be attracted by MHD current to boost the speed of fluid flow.

3.3 Skin Friction and Nusselt Number

The effects of various thermo-physical properties parameters on the dimensionless local skin friction and Nusselt number of MHD flow of ferrofluids are shown in Figure 8 and 9. An increase in ϕ and M parameters has increases the local skin friction and Nusselt number. The variation of the skin friction coefficient C_f (Rex)1/2 and the local Nusselt number Nux (Rex)-1/2 for different values of ϕ and three values of the leading parameter α = 0°, 60°, and 90° in the presence of nanofluids namely Fe_3O_4 – water and Fe_3O_4– kerosene for static plate case are presented in Table 5 and 6. It can be observed that the skin friction increases and Nusselt number decreases, when the volume fraction ϕincreases. Thus, more particles are suspended and thermal conductivity of nanoparticles affected results, skin friction and Nusselt number. It is clear that, the skin friction and the local Nusselt number changes with the change of the nanoparticles volume fraction and magnetic field.

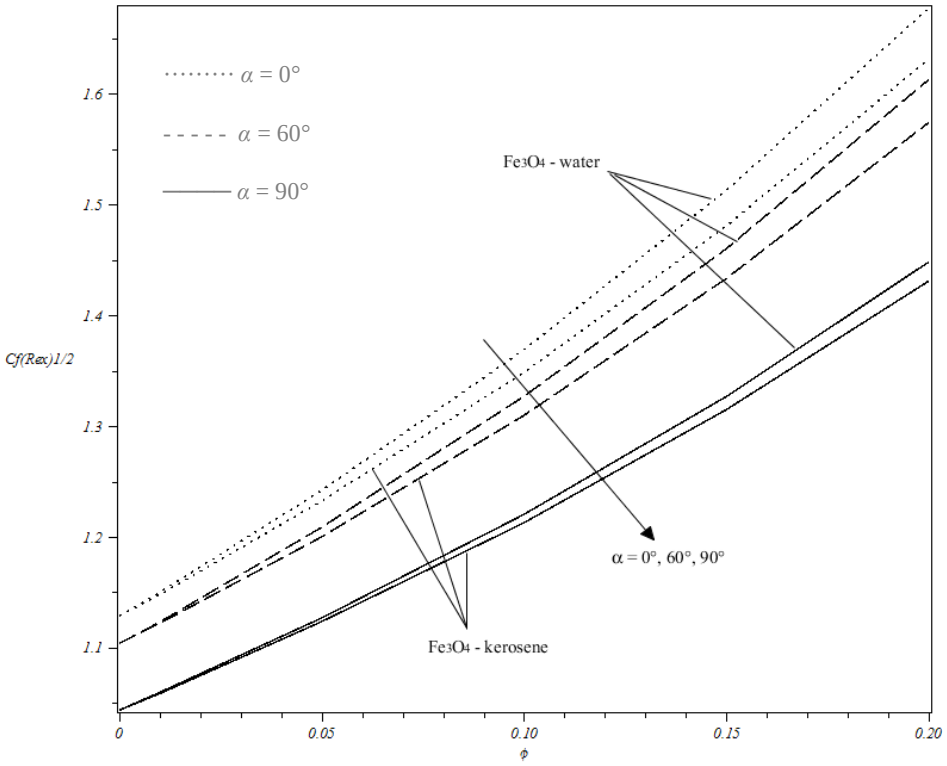

Fig. 8. Variation of the skin friction for different values of leading edge, α with volume fraction, ϕ at M=1

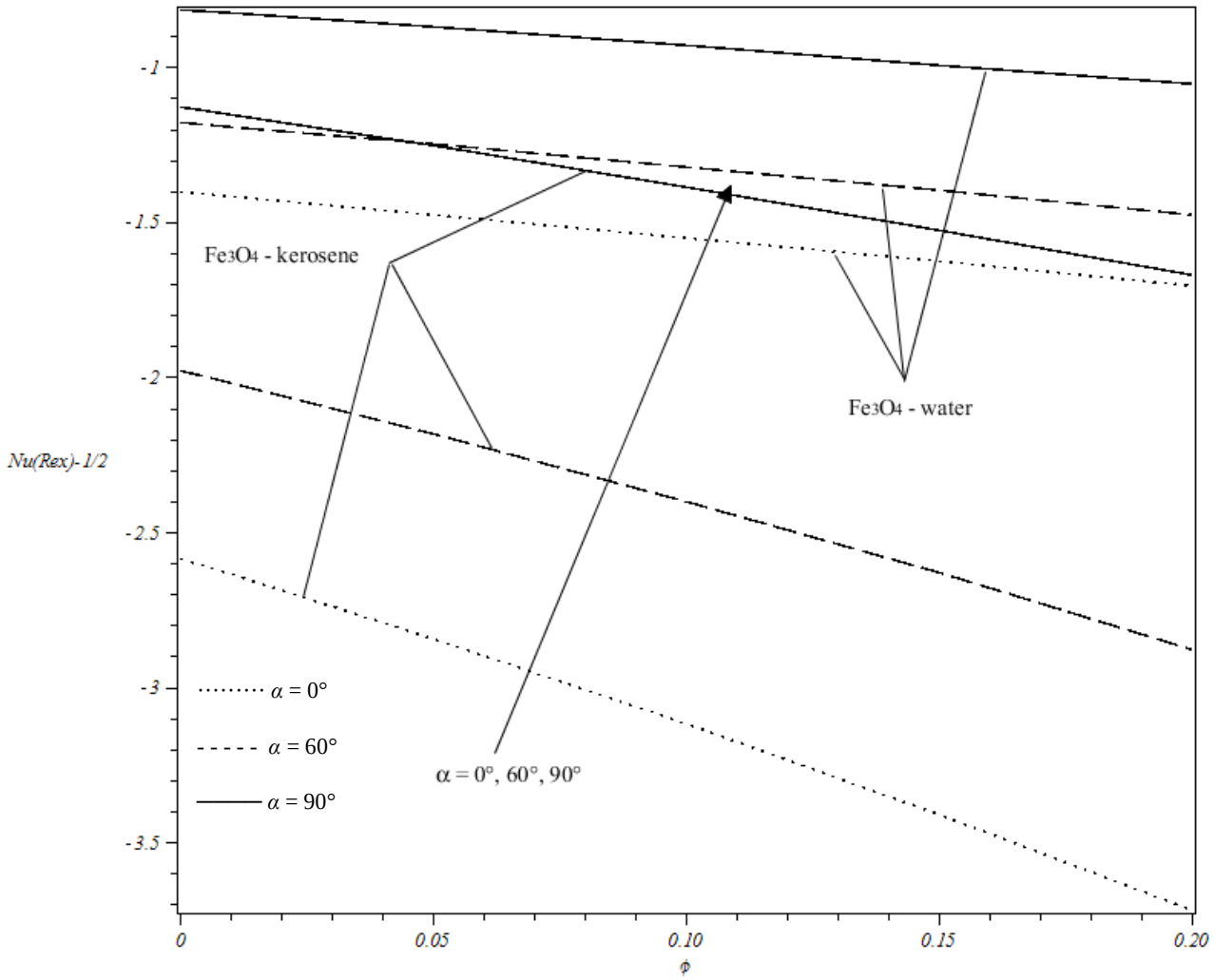

Fig. 9. Variation of the nusselt number for different values of leading edge, α with volume fraction, ϕ at M=1

Table 5 and 6 have shown the important of volume friction (ϕ), magnetic field parameter (M) and leading edge (α) playing a vital role by increasing the skin friction and Nusselt number respectively. Also in Table 5 and 6, it displays results for the skin friction C_f (Rex)1/2 and Nusselt number –Nux (Rex)-1/2 when different parameters are used. It can be seen in Figure 8 that, the lowest skin friction coefficient is obtained for Fe_3O_4 – kerosene at α = 90°. Also in Figure 9, the highest Nusselt number is obtained for Fe_3O_4 – kerosene at α = 0°. The reason is, it has the higher Prandtl number compared to Fe_3O_4– water. In heat transfer problem, the Prandtl number controls the relative thickness of the momentum and thermal boundary layer. In other words, the kerosene base fluid of thermal conductivity is approximately one fourth of water (refer Table 1). Even though water has high thermal conductivity and large heat capacitance which is release a little heat transfer rate compared to kerosene.

Table 5
Variation of skin friction coefficient C_f (Rex)1/2 for Fe_3O_4- water and Fe_3O_4 - kerosene as ferrofluids at different non-dimensional parameters

M	ϕ	Fe_3O_4 - water			Fe_3O_4 - kerosene		
		α			α		
		0°	60°	90°	0°	60°	90°
1	0	1.12837	1.10348	1.04398	1.12837	1.10348	1.04398
1	0.01	1.14811	1.12192	1.05912	1.14999	1.12346	1.05979
1	0.05	1.23179	1.20013	1.12338	1.24161	1.20821	1.12693
1	0.1	1.34831	1.30908	1.21298	1.36902	1.32622	1.22061
1	0.15	1.48041	1.43275	1.31472	1.51326	1.46005	1.32704
1	0.2	1.63127	1.57404	1.43109	1.67775	1.61282	1.44882
1	0.1	1.34831	1.30910	1.21298	1.36902	1.32624	1.22061
2	0.1	1.76026	1.73119	1.66313	1.77539	1.74350	1.66840
3	0.1	2.09533	2.07125	2.01608	2.10769	2.08122	2.02030
5	0.1	2.64280	2.62393	2.58163	2.65230	2.63155	2.58484
10	0.1	3.67203	3.65859	3.62899	3.67868	3.66388	3.63122

Table 6
Variation of reduced Nusselt number -Nux (Rex)-1/2 for Fe_3O_4 - water and Fe_3O_4 - kerosene as ferrofluids at different non-dimensional parameters

M	ϕ	Fe_3O_4 - water			Fe_3O_4 - kerosene		
		α			α		
		0°	60°	90°	0°	60°	90°
1	0	1.40482	1.17807	0.81461	2.58544	1.97935	1.12731
1	0.01	1.41939	1.19235	0.82614	2.63641	2.01968	1.15191
1	0.05	1.47807	1.25003	0.87268	2.84552	2.18522	1.25289
1	0.1	1.55251	1.32353	0.93190	3.11961	2.40241	1.38521
1	0.15	1.62852	1.39882	0.99237	3.40963	2.63231	1.52498
1	0.2	1.70653	1.47612	1.05419	3.71778	2.87655	1.67304
1	0.1	1.55251	1.32353	0.93190	3.11961	2.40241	1.38521
2	0.1	1.55251	1.35143	0.98390	3.11961	2.43580	1.47069
3	0.1	1.55251	1.36992	1.01525	3.11961	2.45913	1.52361
5	0.1	1.55251	1.39446	1.05437	3.11961	2.49166	1.59138
10	0.1	1.55251	1.42808	1.10467	3.11961	2.53950	1.68214

3.4 Effect of Overall Parameters

More clearly in Table 7, has shown overall parameters that affected the velocity and temperature profiles. Meanwhile Table 8 shown overall parameters that affected the skin friction and Nusselt number profiles for both base fluids Fe_3O_4 – water and Fe_3O_4 – kerosene.

Based on physically results, the Fe_3O_4 – kerosene looks better than water that provides a high Prandtl number which influence the isotherms and the streamlines on the heat transfer (see Table 8). Also, kerosene provides a larger Prandtl number that would affect to velocity and temperature behaviour. When Prandtl number is large, decrement of temperature of Fe_3O_4 – kerosene transferred slowly due to increment isothermal lines. However, for small Prandtl number, heat is transferred slower. The Fe_3O_4 – water thermo-physical characteristic is a very good medium of heat capacitance behaviour (Table 7). This is the main reason, all time water is better than kerosene for the

temperature aspect. That proved magnetite particle attracted by MHD current to boost the speed of fluid flow for both base fluids water and kerosene. Examination of heat transfer for the flow of nanofluids shown that the higher Nusselt number is Fe_3O_4 – water compared to Fe_3O_4 – kerosene. The highest Nusselt number is obtained for Fe_3O_4 – water at $\alpha = 0°$ whether increment of volume fraction or magnetic field parameter. The reason is, Fe_3O_4 – water has the higher heat capacitance and thermal conductivity compared to Fe_3O_4 – kerosene. Water base fluid has high thermal conductivity which is more heat transfer rate provided compared to kerosene.

Table 7
Effect of parameters to the velocity f' and the temperature θ with η

Parameters changes	Parameter unchanged (fixed)		Fe_3O_4 – water		Fe_3O_4 – kerosene	
			f'	θ	f'	θ
$\phi \geq 0$ (↑)	M	α	↓(lowest)	↑ (highest)	↓	↑
$\alpha \geq 0°$ (↑)	M	ϕ	↓(lowest)	↑ (highest)	↓	↑
M > 0 (↑)	ϕ	α	↑	↓	↑ (highest)	↓(lowest)

Table 8
Effect of parameters to the skin friction f'' and Nusselt number θ' with η

Parameters changes	Parameter unchanged (fixed)		Fe_3O_4 – water		Fe_3O_4 – kerosene	
			f'	θ	f'	θ
$\phi \geq 0$ (↑)	M	α	↑	↑	↑(highest)	↑(highest)
$\alpha \geq 0°$ (↑)	M	ϕ	↓(lowest)	↓(lowest)	↓	↓
M > 0 (↑)	ϕ	α	↑	↑	↑(highest)	↑(highest)

4. Conclusions

The problem of an unsteady MHD boundary layer flow and heat transfer of ferrofluids over a horizontal flat plate with leading edge accretion has been studied numerically. The governing equations are solved by using similarity transformation with employing the Fourth-Fifth Order Runge-Kutta Felhberg method shooting technique. Graphical results for velocity and temperature are obtained to understand the physical behavior for several embedded parameters. There are two types of base fluids namely water and kerosene are considered with the Prandtl number Pr = 6.2 and 21. The type of nanoparticles used was ferrite material. Ferrite or known as magnetite is a mineral and common naturally-occurring oxides of iron. Based on the numerical results, the following summary is arrived at magnetic field effect when the magnetic parameter increases, it can be seen that the velocity, skin friction and Nusselt number increases which is simultaneously the momentum boundary layer thickness increase. But in temperature, when the magnetic parameter increases, it can be seen that the temperature profiles decrease, which effect also to the decrement of thermal boundary layer thickness.

On the other hand, volume fraction parameter of the nanofluids would be a major effect. It is seen that, nanofluids thermal conductivity increases with increasing particle volume fraction on the temperature profiles, skin friction and Nusselt number although velocity profiles otherwise.

By increasing the leading edge, the velocity profiles, skin friction and Nusselt number decrease when leading edge parameter was increased. Also it has decreased the momentum boundary layer thickness. Temperature profiles found increase with the increasing of leading edge. By increasing the leading edge, it has increased the thermal boundary layer thickness too.

As a result of the review of the nanoparticles impact, it is also found that the presence of nanoparticles is a key factor for the heat enhancement. Pure fluids mixed with nanoparticles are capable of changing the flow and heat transfer capability of the base fluids.

Acknowledgement
The authors would like to thank the My Brains 15 Ministry of Higher Education for financial support. The authors also wish to express their very sincere thanks to reviewer for their valuable comments and suggestions.

References

[1] Saidur, R., K. Y. Leong, and H. A Mohammad. "A review on applications and challenges of nanofluids." *Renewable and sustainable energy reviews* 15, no. 3 (2011): 1646-1668.
[2] Callegari, Andrew J., and Morton B. Friedman. "An analytical solution of a nonlinear, singular boundary value problem in the theory of viscous fluids." *Journal of Mathematical Analysis and Applications* 21, no. 3 (1968): 510-529.
[3] Acrivos, A. "On laminar boundary layer flows with a rapid homogeneous chemical reaction." *Chemical Engineering Science* 13, no. 2 (1960): 57-62.
[4] S.U.S. Choi. "Enhancing thermal conductivity of fluids with nanoparticles." *ASME Publications Fed* 231, (1995): 99-106.
[5] Masuda, Hidetoshi, Akira Ebata, and Kazumari Teramae. "Alteration of thermal conductivity and viscosity of liquid by dispersing ultra-fine particles. Dispersion of Al_2O_3, SiO_2 and TiO_2 ultra-fine particles." *NETSU BUSSEI*, (1993): 227-233.
[6] Alam, Md S., M. M. Rahman, and Md A. Sattar. "Similarity solutions for hydromagnetic free convective heat and mass transfer flow along a semi-infinite permeable inclined flat plate with heat generation and thermophoresis." *Nonlinear Analysis: Modelling and Control* 12, no. 4 (2007): 433-445.
[7] Yamaguchi, H., I. Kobori, Y. Uehata, and K. Shimada. "Natural convection of magnetic fluid in a rectangular box." *Journal of Magnetism and Magnetic materials* 201, no. 1-3 (1999): 264-267.
[8] Albrecht, T., C. Bührer, M. Fähnle, K. Maier, D. Platzek, and J. Reske. "First observation of ferromagnetism and ferromagnetic domains in a liquid metal." *Applied Physics A* 65, no. 2 (1997): 215-220.
[9] Scherer, Claudio, and Antonio Martins Figueiredo Neto. "Ferrofluids: properties and applications." *Brazilian Journal of Physics* 35, no. 3A (2005): 718-727.
[10] Ram, Paras, and Vikas Kumar. "Heat transfer in FHD boundary layer flow with temperature dependent viscosity over a rotating disk." *Fluid Dynamic and Material Processing* 10, no. 2 (2014): 179-196.
[11] Colla, L., L. Fedele, M. Scattolini, and S. Bobbo. "Water-based Fe_2O_3 nanofluid characterization: thermal conductivity and viscosity measurements and correlation." *Advances in Mechanical Engineering* 4 (2012): 674-947.
[12] Abareshi, Maryam, Elaheh K. Goharshadi, Seyed Mojtaba Zebarjad, Hassan Khandan Fadafan, and Abbas Youssefi. "Fabrication, characterization and measurement of thermal conductivity of Fe_2O_4 nanofluids." *Journal of Magnetism and Magnetic Materials* 322, no. 24 (2010): 3895-3901.
[13] Borglin, Sharon E., George J. Moridis, and Curtis M. Oldenburg. "Experimental studies of the flow of ferrofluid in porous media." *Transport in Porous Media* 41, no. 1 (2000): 61-80.
[14] Hiergeist, R., W. Andrä, N. Buske, R. Hergt, I. Hilger, U. Richter, and W. Kaiser. "Application of magnetite ferrofluids for hyperthermia." *Journal of Magnetism and Magnetic Materials* 201, no. 1-3 (1999): 420-422.
[15] Qasim, Muhammad, Zafar Hayat Khan, Waqar Ahmad Khan, and Inayat Ali Shah. "MHD boundary layer slip flow and heat transfer of ferrofluid along a stretching cylinder with prescribed heat flux." *PloS one* 9, no. 1 (2014): e83930.
[16] Khan, Zafar Hayat, Waqar Ahmad Khan, Muhammad Qasim, and Inayat Ali Shah. "MHD stagnation point ferrofluid flow and heat transfer toward a stretching sheet." *IEEE Transactions on Nanotechnology* 13, no. 1 (2013): 35-40.
[17] Malvandi, A., M. H. Kaffash, and D. D. Ganji. "Nanoparticles migration effects on magnetohydrodynamic (MHD) laminar mixed convection of alumina/water nanofluid inside microchannels." *Journal of the Taiwan Institute of Chemical Engineers* 52 (2015): 40-56.
[18] Sheremet, Mikhail A., Ioan Pop, and Natalia C. Roşca. "Magnetic field effect on the unsteady natural convection in a wavy-walled cavity filled with a nanofluid: Buongiorno's mathematical model." *Journal of the Taiwan Institute of Chemical Engineers* 61 (2016): 211-222.

[19] Pourmehran, O., M. Rahimi-Gorji, and D. D. Ganji. "Heat transfer and flow analysis of nanofluid flow induced by a stretching sheet in the presence of an external magnetic field." *Journal of the Taiwan Institute of Chemical Engineers* 65 (2016): 162-171.
[20] Ferdows, M., Md Khan, Md Alam, and Shuyu Sun. "MHD mixed convective boundary layer flow of a nanofluid through a porous medium due to an exponentially stretching sheet." *Mathematical problems in Engineering* 2012 (2012): 1-21.
[21] M.A. Imran. "Heat and Mass Transfer of Magnetohydrodynamic Boundary Layer Stagnation Point Flow of Nanofluid over a Stretching Surface." In Department of Mathematical Sciences, Universiti Teknologi Malaysia, Skudai, Johor, Malaysia., 2013.
[22] Tiwari, Raj Kamal, and Manab Kumar Das. "Heat transfer augmentation in a two-sided lid-driven differentially heated square cavity utilizing nanofluids." *International Journal of Heat and Mass Transfer* 50, no. 9-10 (2007): 2002-2018.
[23] Todd, L. "A family of laminar boundary layers along a semi-infinite flat plate." *Fluid dynamics research* 19, no. 4 (1997): 235-249.
[24] White, Frank M., and Isla Corfield. *Viscous fluid flow*. Vol. 3. New York: McGraw-Hill, 2006.
[25] Brinkman, H. C. "The viscosity of concentrated suspensions and solutions." *The Journal of Chemical Physics* 20, no. 4 (1952): 571-571.
[26] Xuan, Yimin, and Qiang Li. "Heat transfer enhancement of nanofluids." *International Journal of heat and fluid flow* 21, no. 1 (2000): 58-64.
[27] Stewartson, K. "On the impulsive motion of a flat plate in a viscous fluid. II." *The Quarterly Journal of Mechanics and Applied Mathematics* 26, no. 2 (1973): 143-152.
[28] Aziz, Abdul. "A similarity solution for laminar thermal boundary layer over a flat plate with a convective surface boundary condition." *Communications in Nonlinear Science and Numerical Simulation* 14, no. 4 (2009): 1064-1068.
[29] A. Heck. "Solving Equations, in: Introduction to Maple." *Springer, New York*, (2003): 481-520.
[30] Parasuraman Loganathan, Chellasamy Vimala. "Unsteady boundary layer flow and heat transfer of a nanfoluid past a static and moving flat plate." *International Journal of Heat and Technology* 31, no. 2 (2013): 95-102.
[31] Blasius, Heinrich. "Das aehnlichkeitsgesetz bei reibungsvorgängen in flüssigkeiten." In *Mitteilungen über Forschungsarbeiten auf dem Gebiete des Ingenieurwesens*, pp. 1-41. Springer, Berlin, Heidelberg, 1913.
[32] Cortell, Rafael. "Numerical solutions of the classical Blasius flat-plate problem." *Applied Mathematics and Computation* 170, no. 1 (2005): 706-710.